Available online at www.sciencedirect.com
SciVerse ScienceDirect
Ceramics International 39 (2013) 4559–4567
CERAMICS INTERNATIONAL
www.elsevier.com/locate/ceramint

A green sol–gel route for the synthesis of structurally controlled silica particles from rice husk for dental composite filler

Noor Sheeraz Che Zulkifli, Ismail Ab Rahman*, Dasmawati Mohamad, Adam Husein

School of Dental Sciences, Universiti Sains Malaysia, 16150 Kubang Kerian, Kelantan, Malaysia

Received 17 October 2012; received in revised form 20 November 2012; accepted 20 November 2012
Available online 23 December 2012

Abstract

A green sol–gel route for preparing structurally controlled non-crystalline silica particles from rice husk was developed. At optimal conditions, amorphous spherical silica particles with a surface area of $\sim 364\ \mathrm{m^2\,g^{-1}}$ and particle sizes ranging from 75 to 252 nm were synthesised through the addition of phosphoric acid into sodium silicate derived from rice husk. The powder was mesoporous with a pore size of ~8 nm. It was observed that the degree of agglomeration of the powder was highly dependent on the sodium silicate precursor concentration, pH and solvent. TEM, SEM, N_2 adsorption/desorption, XRD and FTIR techniques were used to characterise the silica powder. The route developed is simple and environmental friendly and could help solve pollution problems. The silica produced is suitable for use as a filler in dental restoration composites.

Keywords: Rice husk; Sol–gel; Spherical silica; Filler

1. Introduction

Recent progress in the synthesis of spherical nanosilica based on the sol–gel technique has significantly boosted the development of silica–polymer nanocomposites. Silica particles with different particle sizes and morphologies been produced via the sol–gel technique by controlling parameters such as the concentration of alkoxide, amount of water, pH, solvent and aging time [1–7]. However, the synthesis route is time consuming and costly and involves toxicity exposure from silicon alkoxide precursors.

In continuing attempts to reduce processing cost and time, many research works have been published on the use of rice husk as a raw material for producing silica nanoparticles [8–14]. Rice husk that contains ~20% silica is abundantly available in rice-producing countries and provides a low-cost silica source. Currently, rice husk is primarily burned to obtain valuable silica, but that will cause air pollution because it releases a large number of greenhouse gases, and the emission of rice husk ash into the ecosystem results in silicosis syndrome, fatigue, shortness of breath, loss of appetite and respiratory failure [15]. Thus, the extraction of silica from rice husk in a more benign manner is becoming important as society strives towards the quality and environmental preservation through sustainable development and the use of cleaner technology [16]. Without specific applications in mind, various methods have been developed for preparing silica from rice husk. Recently, highly porous silica has been produced using pyrolysed rice husk in less than 10 h using polyethylene glycol (PEG) as a template [17]. Another study produced sphere-like nanosilica with an average diameter of ~51 nm from rice husk by using simple sol–gel synthesis [18]. The activated carbon extracted from rice husk has been used for the preparation of sphere-like silica powder with diameters of 30–200 nm [19,20]. Bimodal porous silica synthesised from rice husk ash by using chitosan as a template has also been reported [21]. However, no work has been reported for the preparation of silica particles with well-defined morphologies from rice husk that does not require any expensive templates or consume a large amount of energy. Thus, silica powder has not been appropriate for dental filler applications. It would be beneficial to develop a simple, economical process that uses a low-energy method to

---

*Corresponding author. Tel.: +609 7675 818; fax: +609 7642 026.
E-mail address: arismail@usm.my (I. Ab Rahman).

0272-8842/$ - see front matter © 2012 Elsevier Ltd and Techna Group S.r.l. All rights reserved.
http://dx.doi.org/10.1016/j.ceramint.2012.11.052

produce silica powder with controlled morphologies from rice husk, thereby utilising waste for an economically value-added product.

In this study, the synthesis of silica nanoparticles with spherical structures through the sol–gel route using a sodium silicate precursor derived from rice husk is reported. Phosphoric acid is used as the precipitating agent due to its polyprotic property that can control the hydrolysis reaction and particle formation. In addition, this acid is commonly used as an additive in food industries, medicine and dentistry. A systematic study of the parameters that affect the formation of silica particles has been carried out. The physical and chemical properties of silica were investigated to determine its feasibility as a low-cost biomaterial filler for dental restoration applications.

2. Experimental

2.1. Materials and reagents

Rice husk was obtained from a rice mill in Kelantan, Malaysia. Phosphoric acid (85%), hydrochloric acid (37%) and absolute ethanol (99.5%) were purchased from Sigma-Aldrich. Sodium hydroxide (99%) was purchased from Merck in pellet form. All chemicals used were AR grades, and distilled water was used for all synthesis and treatment processes.

2.2. Preparation of sodium silicate

First, rice husk was treated with diluted HCl in a water bath at 75 °C for 4 h to remove metallic impurities. The suspension was filtered and the solid residue was repeatedly washed with distilled water until the filtrate was free of the acid (pH of filtrate ~7). The residue was then dried at 110 °C for 12 h in an oven. A known amount of dried rice husk was added to a Teflon flask containing 10 wt% NaOH and boiled at 90 °C for 1 h with constant stirring. Then, the mixture was subsequently cooled at room temperature and filtered to obtain sodium silicate (SS) with a specific gravity of 1.13.

2.3. Synthesis of silica particles

The silica particle synthesis procedure is schematically illustrated in Fig. 1. Different amounts of ethanol were mixed with sodium silicate. Then, water was added and stirred for 10 min. The mixture was slowly titrated with 3 M H_3PO_4 until the gel was formed at pH values of 7, 8 and 9. Then, the yellowish gel was centrifuged and washed eight times with hot distilled water to remove any excess sodium silicate and phosphate. The sample was dried in a freeze dryer and finally calcined in a furnace to obtain the silica powder.

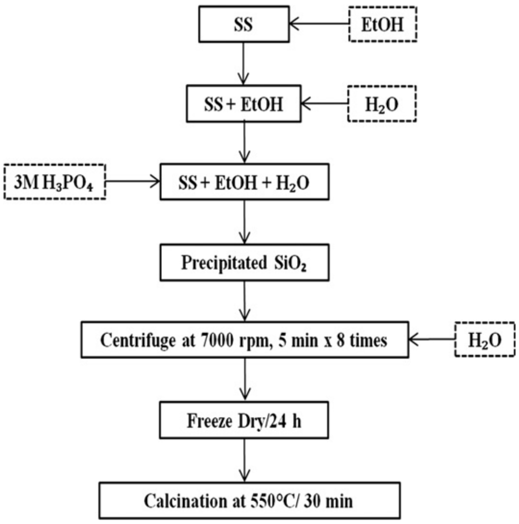

Fig. 1. Flow chart of silica synthesis using a sodium silicate precursor derived from rice husk. (SS=Sodium silicate; EtOH=Ethanol).

2.4. Characterisation

Transmission electron micrographs were obtained from a transmission electron microscopy (TEM, Philips FEI CM12) system and the particle size was measured using analySIS Docu Version 3.2 image processing software. A field-emission scanning electron microscope equipped with energy-dispersive X-ray (EDX) (FE-SEM, Quanta FEG450) was used to analyse the silica particles. The N_2 adsorption/desorption isotherms were measured by an automatic surface area and pore size analyser (Quantacerome AUTOSORB-1) at 77 K. The specific surface area was determined by using BET equation. A single point total pore volume was estimated as the liquid volume of N_2 adsorbed at a relative pressure of 0.1 and 0.97, respectively. A Fourier Transform Infrared (FTIR) spectrum (Perkin-Elmer 2000) was obtained from a pellet composed of a mixture of sample and spectroscopic-grade KBr at a mass ratio of ~1/100 that was analysed over the wave number range of 4000–400 cm^{-1}. X-ray diffraction (XRD) patterns were obtained from an X-ray diffractometer (Philip Electronic Instruments) using an acceleration voltage of 30 kV and a current of 160 mA. The diffraction angle was scanned from 10° to 80° 2θ at 8° min^{-1}.

3. Results and discussion

3.1. Synthesis of silica particles

The synthesis of silica particles from rice husk was previously reported by other researchers [10–12,17–20]. However, the silica powders produced were nanosized and composed of various structures (porous and agglomerate) without specific applications. In this work, silica powder was produced from rice husk through the sol–gel route by using phosphoric acid as the precipitating agent.

The synthesised powder possesses desirable chemical and physical properties and has a high potential for use in dental composite preparation, which will be explored in our future work.

Sodium silicate as a precursor was obtained by reacting rice husk and sodium hydroxide. In principle, the route for obtaining silica powder is identical to the precipitation process using inorganic acids such as HNO_3 [18], HCl [22,23] and H_2SO_4 [24]. By using phosphoric acid as a precipitating agent, the overall reaction can be represented as:

$$3Na_2SiO_3 + 2H_3PO_4 \rightarrow 3SiO_2 + 2Na_3PO_4 + 3H_2O \tag{1}$$

During the addition of phosphoric acid, the ≡Si–OH species formed and condensed together to form siloxane [Si–O–Si] bonds as represented below:

$$\equiv\text{Si–OH} + \text{HO–Si}\equiv \; \rightarrow \; \equiv\text{Si–O–Si}\equiv + H_2O \tag{2}$$

At the initial stage, the ≡Si–OH species may form dimmers or trimers or grow into primary particles [6]. The aggregation of primary particles results in more stable particles. The formation of different particle morphologies was highly dependent on the reaction condition that was investigated in the present work.

3.1.1. Effect of the addition of ethanol

TEM micrographs of silica particles prepared through the addition of different amounts of ethanol are shown in Fig. 2. Without ethanol, the particles were highly agglomerated and irregular in shape (Fig. 2a). Spherical and more dispersed particles are observed with increasing amount of ethanol (Fig. 2b,c). This may be due to the high miscibility of ethanol that accelerates the penetration into the silicate precursor. This behaviour enhances the formation of ≡Si–OH and ≡Si–O–Si≡ that produces more spherical and larger particles during the aging process [25,26].

The results in Table 1 showed that the BET surface areas were reduced from ~301 to ~73 $m^2\,g^{-1}$ with increases in the addition of ethanol. A higher specific surface area of silica particles without ethanol (sample 1:0:0) may be attributed to the porous particulates of three-dimensional cross-linking silica networks. However, under these conditions, the shape of the particles is irregular, and it is difficult to measure the size of particles (Fig. 2a).

3.1.2. Effect of pH

In the preparation of silica gel, pH is also a critical parameter in determining the particle size and morphology of the silica particles [27]. In this work, pH was controlled by the slow addition of diluted phosphoric acid. At a fixed

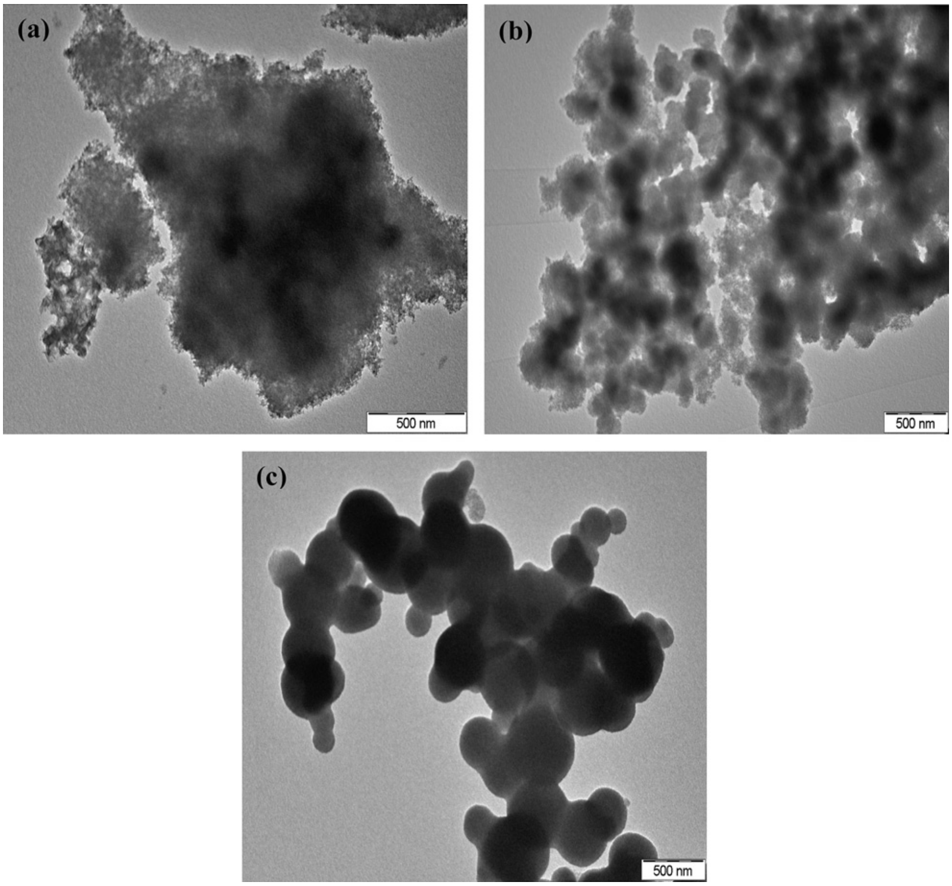

Fig. 2. TEM images of the silica prepared at different amounts of ethanol based on ratio of SS:H_2O:EtOH at pH 9: (a) 1:0:0 (b) 1:0:0.15 (c) 1:0:0.25.

Table 1
The BET surface area, single point total pore volume, average pore diameter and particle size of the silica samples prepared at different parameters.

Samples	BET surface area ($m^2\,g^{-1}$)	Single point total pore volume ($cm^3\,g^{-1}$)	Average pore diameter (nm)	Average particle size (nm)	Particle size range (nm)
Effect of Ethanol					
1:0:0[a]	300.82	1.17	15.56	NA	NA
1:0:0.15[a]	197.66	0.48	9.72	180.67	98–272
1:0:0.25[a]	73.26	0.14	7.64	288.49	94–631
Effect of pH					
pH 7[b]	196.66	0.24	4.89	226.37	78–435
pH 8[b]	198.49	0.32	6.50	294.79	51–607
Effect of addition of water					
1:1:0.25[c]	364.35	0.72	7.92	147.49	75–252
1:1:0.25[d]	357.86	0.67	7.68	164.49	37–267
1:1:0.25[e]	212.45	1.21	7.7	192.00	28–317

[a] Samples were prepared using 3 M H_3PO_4 at pH 9 based on ratio of SS:H_2O:EtOH.
[b] Samples were prepared using 3 M H_3PO_4 based on ratio of SS:H_2O:EtOH = 1:0:0.25.
[c] Samples were prepared using 3 M H_3PO_4 at pH 7 based on ratio of SS:H_2O:EtOH.
[d] Samples were prepared using 3 M H_3PO_4 at pH 8 based on ratio of SS:H_2O:EtOH.
[e] Samples were prepared using 3 M H_3PO_4 at pH 9 based on ratio of SS:H_2O:EtOH.

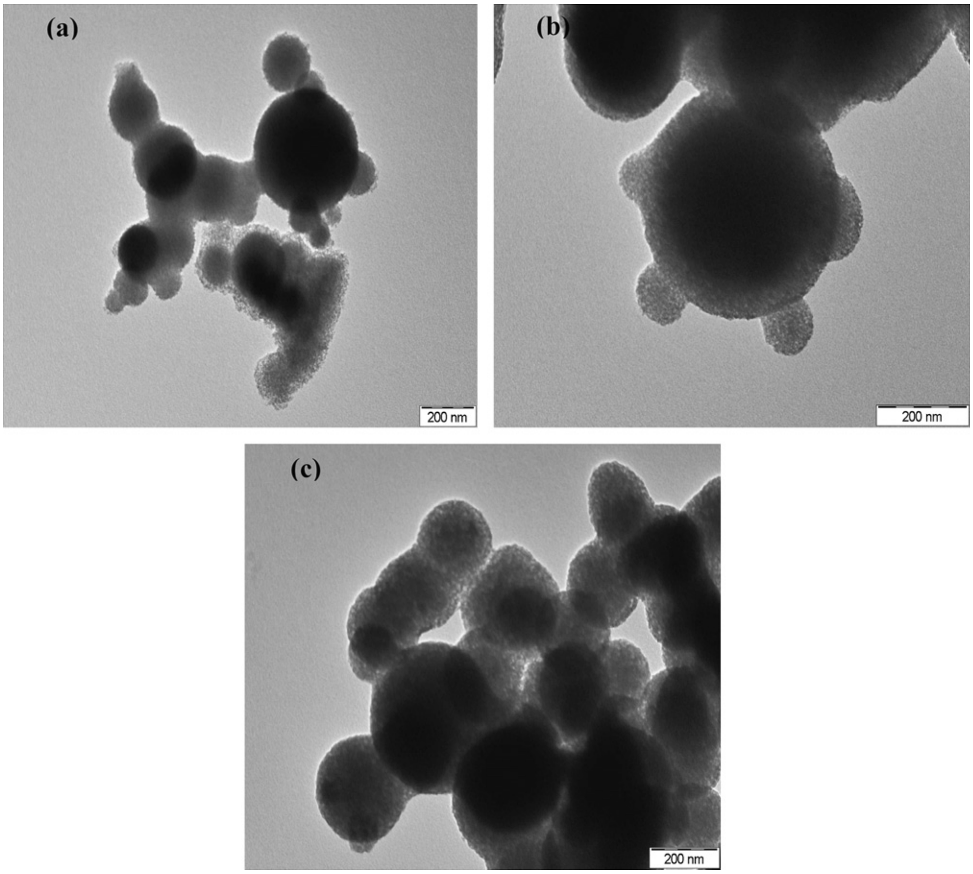

Fig. 3. TEM images of the silica prepared at different pH based on the ratio of SS:H_2O:EtOH = 1:0:0.25 at pH: (a) 7 (b) 8 (c) 9.

ethanol ratio and silicate concentration, the particle size increased with increases in the pH. TEM micrographs of the silica particles are shown in Fig. 3. The results showed that the morphologies of silica particles were more spherical in shape and that the particle size increased and was more widely distributed as the pH increased. A higher pH results in higher hydrolysis and condensation rates (reactions (3) and (4)) that promote growth and the formation of spherical particles [22]. At $pH > 9$, hard gel is formed immediately after the addition of phosphoric acid, leading to hard agglomerated particles. At $pH < 7$, the suspension become very dilute and ageing took more than 2 days, which is not feasible for the preparation of silica. Thus, the pH range used in this work is 7–9.

$$\equiv Si\text{–}OH + OH^- \rightarrow \equiv Si\text{–}O^- + H_2O \tag{3}$$

$$\equiv Si\text{–}OH + \equiv Si\text{–}O^- \rightarrow \equiv Si\text{–}O\text{–}Si\equiv + OH^- \tag{4}$$

By analysing N_2 adsorption/desorption isotherms, the BET surface areas of silica were determined to be ~ 197, ~ 198 and $\sim 73\ m^2\ g^{-1}$ with corresponding pore diameters of 4.89, 6.50 and 7.64 nm obtained at pH 7, 8 and 9, respectively (Table 1). The decrease in surface area corresponds to an increase in particle size as discussed earlier. According to the IUPAC classification, the prepared silica gels can be classified as mesoporous materials because the pore size was in the range of 2–50 nm [22,27].

3.1.3. *Effect of the addition of water*

In this work, sodium silicate is a source of $\equiv Si\text{–}OH$ species. Thus, its concentration will affect reactions (2), (3) and (4) and determine the degree of agglomeration of silica particles. Fig. 4 shows the effect of the addition of water on the morphologies and size of silica particles. At a high concentration of sodium silicate, the particles are highly agglomerated due to the large amount of hydrolysed species, which resulted in extensive growth of primary particles. After dilution with water, the size of the silica particles was smaller, the particles were more disperse and there were fewer aggregates (Fig. 4b). In this condition, the concentration of silicate is reduced. Limiting condensation reaction results in slower particle growth and reduces the particle size. The results in Table 1 showed that the average size of silica particles decreased from 226.37 to 147.49 nm at pH 7 (sample, SS:EtOH = 1:0.25). Consequently, the specific surface area and pore diameter were increased from 196.66 to 364.35 $m^2\ g^{-1}$ and from 4.89 to 7.92 nm, respectively, under $SS:H_2O:EtOH = 1:0:0.25$ and 1:1:0.25.

3.2. *Pore structure analysis*

Fig. 5 shows typical nitrogen adsorption–desorption isotherms of silica particles produced under various

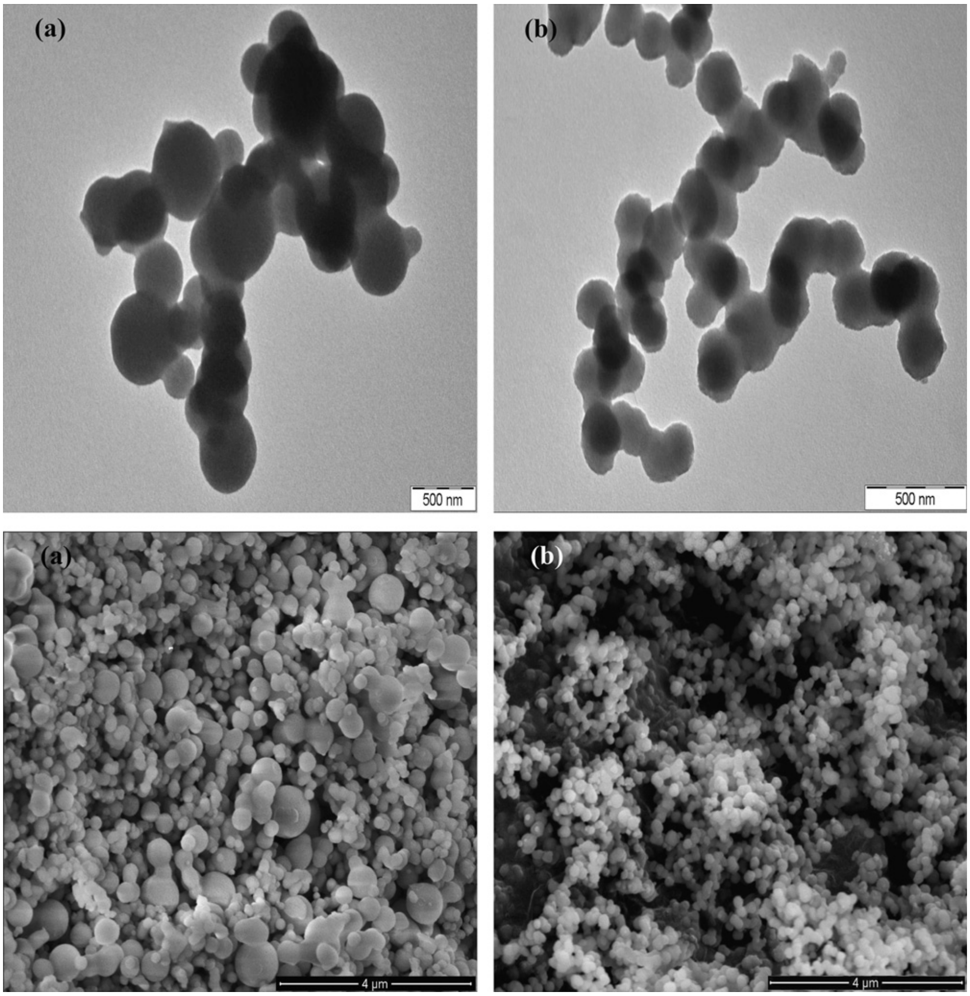

Fig. 4. TEM versus SEM images of the silica prepared at different amounts of water based on the ratio of $SS:H_2O:EtOH$ at pH 8: (a) 1:0:0.25 (b) 1:1:0.25.

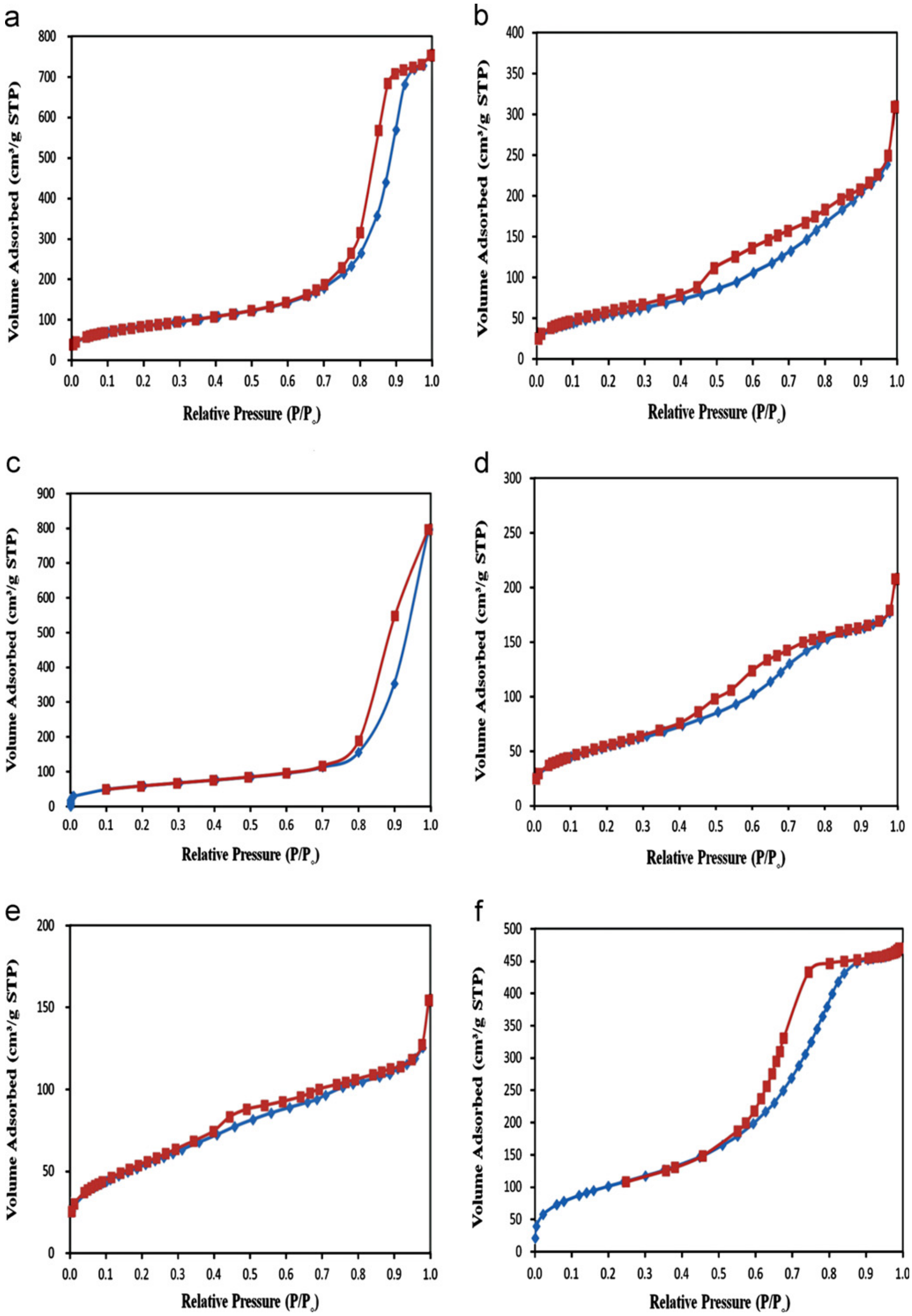

Fig. 5. N_2 adsorption/desorption isotherms of various silica prepared at different ratio of SS:H_2O:EtOH and pH: (a) 1:0:0 pH 9 (b) 1:0:0.15 pH 9 (c) 1:0:0.25 pH 9 (d) 1:0:0.25 pH 8 (e) 1:0:0.25 pH 7 (f) 1:1:0.25 pH 7.

conditions. Most of the isotherms belonged to the type IV category in the IUPAC classification of different types of hysteresis loops. The type IV isotherm shape is generally associated with mesoporous adsorbents [28]. Fig. 5a and f show that the type IV isotherm consists of a narrow H1 hysteresis loop with very steep and parallel adsorption and desorption branches that are associated with adsorbents with a narrow and uniform pore distribution. Fig. 5b, d and e show the H2-type hysteresis broad loop with a gradual uptake in adsorption and a very steep desorption branch. This type is typically observed with porous materials having networks of interconnected pores of progressive sizes and shapes. Fig. 5c shows a type II isotherm for nonporous solids. The type of hysteresis loop corresponds to the H4 type which is associated with narrow slit-like pores. All of the isotherms are closely related to the morphological properties of the prepared powders.

Fig. 6 shows the pore size distribution from the adsorption of nitrogen isotherm at various conditions estimated by the BJH model. The pore size of silica decreased as the amount of ethanol increased. The sample SS:H_2O:EtOH = 1:0:0 displays a narrow distribution curve, which may be due to the particulate nature of silica (Fig. 2a). Other samples show broad peaks at pore diameters in the range of 4.89–9.72 nm. However, the pore sizes of all samples were between 2 and 50 nm, indicating that the silica produced contained a high proportion of mesopores [22,27].

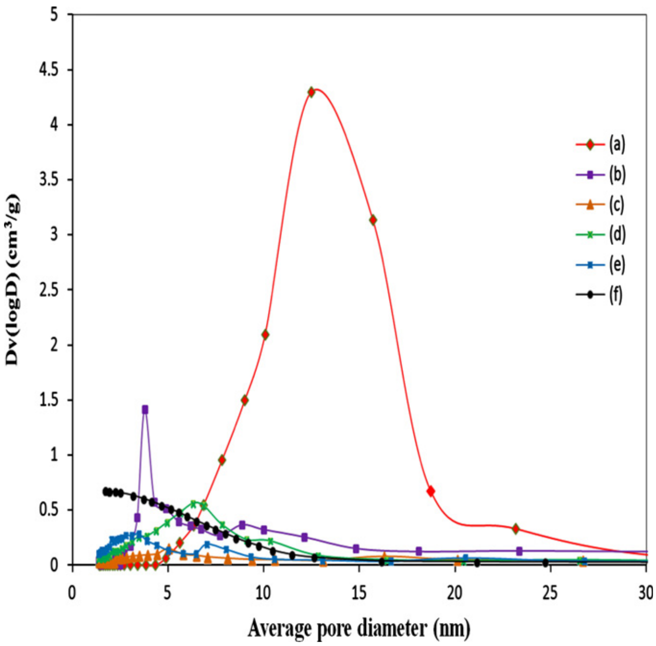

Fig. 6. BJH pore size distribution curve computed from the adsorption isotherm of various silica prepared at different ratio of SS:H_2O:EtOH and pH: (a) 1:0:0 pH 9 (b) 1:0:0.15 pH 9 (c) 1:0:0.25 pH 9 (d) 1:0:0.25 pH 8 (e) 1:0:0.25 pH 7 (f) 1:1:0.25 pH 7.

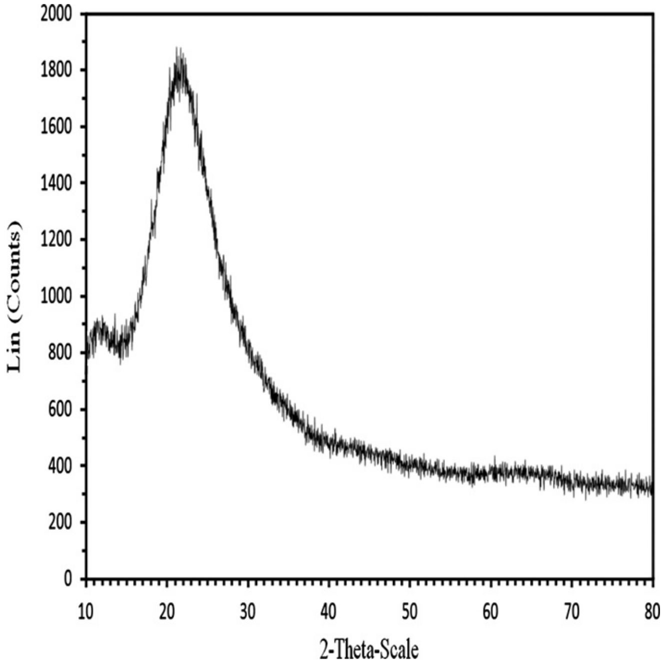

Fig. 7. XRD pattern of the silica sample produced from rice husk.

3.3. *Analysis of FTIR and XRD*

The XRD characteristic absorption peaks of the silica particles are shown in Fig. 7. The result shows a broad and high intensity peak at 22° (2θ) which is typical for the amorphous nature of silica [23] and which was confirmed by the absence of an ordered crystalline structure.

Fig. 8 presents the infrared spectra of the silica that was examined by FTIR spectroscopy in the range of 4000–400 cm^{-1}, and the major chemical groups of silica are identified. The predominant absorbance peaks at

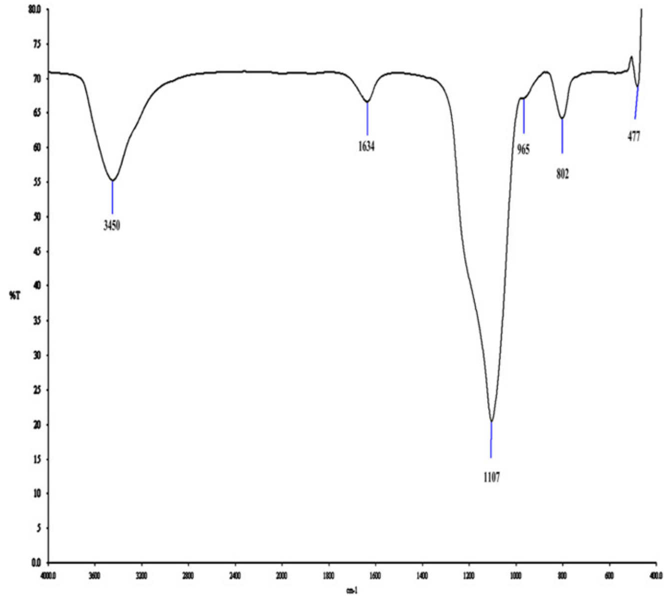

Fig. 8. FTIR spectrum of the silica sample produced from rice husk.

Table 2
Experimental parameters at the optimum conditions.

Parameters	**Variations**	**Optimal value**
Ethanol	0–0.25	0.25
pH	7–9	7
Dilution	0–1	1

Table 3
EDX analysis of the silica powder prepared under conditions: SS:H_2O:EtOH = 1:1:0.25, pH 7.

Element	**Average weight %**
O	58.56
Na	0.64
Si	40.80
Total	100.00

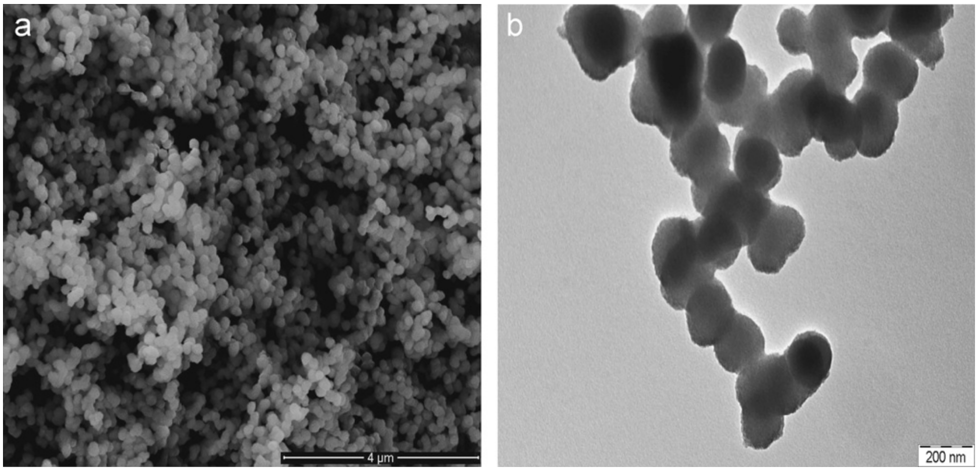

Fig. 9. (a) SEM and (b) TEM images of the silica particles prepared at optimal experimental conditions.

1107 cm^{-1} correspond to the asymmetric vibrations of the siloxane bond, Si–O–Si. The bands located at 802 cm^{-1} and 477 cm^{-1} are assigned to the Si–O symmetry stretching vibration and bending vibration, respectively. The band at approximately 3450 cm^{-1} and 965 cm^{-1} is ascribed to the SiO–H asymmetry stretching vibration and bending vibration, respectively. The band at 1634 cm^{-1} belonged to the –OH stretching vibration of the silanol or adsorbed water molecules on the silica surface [29].

3.4. Synthesis of silica particles under optimised conditions

The optimal conditions for the synthesis of spherical particles were determined and are listed in Table 2. Fig. 9 shows micrographs of the particles. The images reveal a uniform morphology with low aggregation. The powder shows the highest BET surface area of ~364 m^2 g^{-1} with particle sizes ranging from 75 to 252 nm. The powder was considered a mesoporous material because the size of the pore was 7.92 nm (sample 1:1:0.25 at pH 7, Table 1). The size of the produced silica particle is within the range of the filler size that is typically used in dental composition [30,31].

Table 3 shows the EDX analysis. The presence of oxygen (O), sodium (Na) and silicon (Si) were detected in silica powder. The presence of Si and O was due to the formation of siloxane bonds (Si–O–Si) and silanol groups (Si–OH). A small amount of sodium was detected because the phosphoric acid could not dissolve all Na$^+$ ions from sodium silicate solution. No trace of phosphate was detected in the sample, which may be because either all phosphate was consumed during precipitation or was washed out during the washing process.

4. Conclusions

Spherical silica particles were synthesised from rice husk using a sodium silicate precursor derived from rice husk. By controlling reaction conditions such as with the addition of ethanol, by changing of the pH (phosphoric acid) and with addition of water, a high specific surface area of ~364 m^2 g^{-1} and spherical morphology were obtained. This cheap and environmentally friendly route produced silica particles with desirable properties that have the potential to be used in dental composites.

Acknowledgements

The author would like to thank Universiti Sains Malaysia for funding this research through the RU Grant no. 1001/PPSG/814110. Noor Sheeraz Che Zulkifli would like to express her gratitude to the Malaysian Government for financial support under the My Brain 15 programme.

References

[1] W. Stöber, A. Fink, E. Bohn, Controlled growth of monodisperse silica spheres in the micron size range, Journal of Colloid and Interface Science 26 (1968) 62–69.
[2] J.K. Bailey, M.L. Mecartney, Formation of colloidal silica particles from alkoxides, Colloids and Surfaces 63 (1992) 151–161.
[3] S.K. Park, K.D. Kim, H.T. Kim, Preparation of silica nanoparticles: determination of the optimal synthesis conditions for small and uniform particles, Colloids and Surfaces A: Physicochemical Engineering Aspects 197 (2002) 7–17.
[4] D.L. Green, J.S. Lin, Y.-F. Lam, M.Z.C. Hu, D.W. Schaefer, M.T. Harris, Size, volume fraction, and nucleation of Stober silica nanoparticles, Journal of Colloid and Interface Science 266 (2003) 346–358.
[5] I.A. Rahman, P. Vejayakumaran, C.S. Sipaut, J. Ismail, M. Abu Bakar, R. Adnan, C.K. Chee, Effect of anion electrolytes on the formation of silica nanoparticles via the sol–gel process, Ceramics International 32 (2006) 691–699.
[6] I.A. Rahman, P. Vejayakumaran, C.S. Sipaut, J. Ismail, M.A. Bakar, R. Adnan, C.K. Chee, An optimized sol–gel synthesis of stable primary equivalent silica particles, Colloids and Surfaces A: Physicochemical Engineering Aspects 294 (2007) 102–110.
[7] K.D. Kim, K.Y. Choi, J.W. Yang, Formation of spherical hollow silica particles from sodium silicate solution by ultrasonic spray pyrolysis method, Colloids and Surfaces A: Physicochemical Engineering Aspects 254 (2005) 193–198.

[8] S. Huang, S. Jing, J. Wang, Z. Wang, Y. Jin, Silica white obtained from rice husk in a fluidized bed, Powder Technology 117 (2001) 232–238.

[9] Q. Tang, T. Wang, Preparation of silica aerogel from rice hull ash by supercritical carbon dioxide drying, Journal of Supercritical Fluids 35 (2005) 91–94.

[10] D. An, Y. Guo, B. Zou, Y. Zhu, Z. Wang, A study on the consecutive preparation of silica powders and active carbon from rice husk ash, Biomass and Bioenergy 35 (2011) 1227–1234.

[11] Y. Liu, Y. Guo, Y. Zhu, D. An, W. Gao, Z. Wang, Y. Ma, Z. Wang, A sustainable route for the preparation of activated carbon and silica from rice husk ash, Journal of Hazardous Materials 186 (2011) 1314–1319.

[12] L. Dawei, Z. Xifeng, Short-period synthesis of high specific surface area silica from rice husk char, Materials Letters 65 (2011) 1528–1530.

[13] J. Schlomach, M. Kind, Investigations on the semi-batch precipitation of silica, Journal of Colloid and Interface Science 277 (2004) 316–326.

[14] U. Kalapathy, A. Proctor, J. Shultz, A simple method for production of pure silica from rice hull ash, Bioresource Technology 73 (2000) 257–262.

[15] K.Y. Foo, B.H. Hameed, Utilization of rice husk ash as novel adsorbent: a judicious recycling of the colloidal agricultural waste, Advance Colloid and Interface Science 152 (2009) 39–47.

[16] S. Yusoff, Renewable energy from palm oil-innovation on effective utilization of waste, Journal of Cleaner Production 14 (2006) 87–93.

[17] L. Dawei, D. Chen, X. Zhu, Reduction in time required for synthesis of high specific surface area silica from pyrolyzed rice husk by precipitation at low pH, Bioresource Technology 102 (2011) 7001–7003.

[18] F. Adam, T.S. Chew, J. Andas, A simple template-free sol–gel synthesis of spherical nanosilica from agricultural biomass, Journal of Sol–Gel Science and Technology 59 (2011) 580–583.

[19] H. Zhang, X. Zhao, X. Ding, H. Lei, X. Chen, D. An, Y. Li, Z. Wang, A study on the consecutive preparation of d-xylose and pure superfine silica from rice husk, Bioresource Technology 101 (2010) 1263–1267.

[20] Y. Li, X. Ding, Y. Guo, C. Rong, L. Wang, Y. Qu, X. Ma, Z. Wang, A new method of comprehensive utilization of rice husk, Journal of Hazardous Materials 186 (2011) 2151–2156.

[21] T. Witoon, M. Chareonpanich, J. Limtrakul, Size control of nanostructured silica using chitosan template and fractal geometry: effect of chitosan/silica ratio and aging temperature, Journal of Sol–Gel Science and Technology 56 (2008) 270–277.

[22] T.-H. Liou, C.-C. Yang, Synthesis and surface characteristics of nanosilica produced from alkali-extracted rice husk ash, Materials Science and Engineering B 176 (2011) 521–529.

[23] M. Rozainee, S.P. Ngo, A.A. Salema, K.G. Tan, Fluidized bed combustion of rice husk to produce amorphous siliceous ash, Energy for Sustainable Development 12 (2008) 33–42.

[24] N. Pijarn, A. Jaroenworaluck, W. Sunsaneeyametha, R. Stevens, Synthesis and characterization of nanosized-silica gels formed under controlled conditions, Powder Technology 203 (2010) 462–468.

[25] C.Y. Jung, J.S. Kim, T.S. Chang, S.T. Kim, H.J. Lim, S.M. Koo, One-step synthesis of structurally controlled silicate particles from sodium silicates using a simple precipitation process, Langmuir 26 (2010) 5456–5461.

[26] R.H.M. Godoi, L. Fernandes, M. Jafelicci Jr., R.C. Marques, L.C. Varanda, M.R. Davolos, Investigation of the systems silica and silica containing chromium in alcohol medium, Journal of Non-Crystalline Solids 247 (1999) 141–145.

[27] U. Kalapathy, A. Proctor, J. Shultz, Silica xerogels from rice hull ash: structure, density and mechanical strength as affected by gelation pH and silica concentration, Journal of Chemical Technology and Biotechnology 75 (2000) 464–468.

[28] K.S.W. Sing, D.H. Everett, R.A.W. Haul, L. Moscou, R.A. Pierotti, J. Rouquerol, T. Siemieniewska, Reporting Physisorption Data for Gas/Solid Systems Handbook of Heterogeneous Catalysis, Wiley-VCH Verlag GmbH & Co. KGaA, 2008.

[29] P.K. Jal, M. Sudarshan, A. Saha, S. Patel, B.K. Mishra, Synthesis and characterization of nanosilica prepared by precipitation method, Colloids and Surfaces A: Physicochemical Engineering Aspects 240 (2004) 173–178.

[30] M. Kaleem, J.D. Satterthwaite, D.C. Watts, Effect of filler particle size and morphology on force/work parameters for stickiness of unset resin-composites, Dental Materials 25 (2009) 1585–1592.

[31] K. Fujita, T. Ikemi, N. Nishiyama, Effects of particle size of silica filler on polymerization conversion in a light-curing resin composite, Dental Materials 27 (2011) 1079–1085.